ARTIFICIAL SATELLITES, Vol. 57, No. 4 – 2022
DOI: 10.2478/arsa-2022-0011

INVESTIGATION OF SIGNALS OF THE RANGE 10^{-3}–10^{-4} Hz REGISTERED BY WATER-TUBE TILTMETERS IN THE UNDERGROUND GEODYNAMIC LABORATORY IN KSIĄŻ (SW POLAND)

Marek KACZOROWSKI[1], Damian KASZA[2], Ryszard ZDUNEK[1], Roman WRONOWSKI[1]

[1] Space Research Centre, Polish Academy of Sciences, Warsaw, Poland
[2] Faculty of Geoengineering, Mining and Geology, Wrocław University of Science and Technology, Wrocław, Poland

e-mail: damian.kasza@pwr.edu.pl

ABSTRACT. The Geodynamic Laboratory in Książ includes investigations of various kinds of geodynamic signals. Among others, we registered harmonic signals of the range 10^{-3}–10^{-4} Hz. These signals had been found in the measurement series of the long water-tube (WT) tiltmeters. The discovered signals consist of two classes of harmonics associated with various kinds of phenomena. The first class of these signals belongs to viscoelastic vibrations of the Earth's solid body, while the second class is produced possibly by the extremely long atmospheric infrasound waves. The signals of the vibrations of the Earth had been well recognized by the characteristic frequencies of the Earth's free vibrations' resonance, which occur mainly after strong earthquakes. The atmospheric pressure microvibrations affected the water level in the hydrodynamic systems of the WTs as a result of an inverse barometric effect. We observed that signals from both classes blend in the harmonics of similar frequencies and jointly affect the hydrodynamic systems of the WTs. We found that the amplitude of the second-class signals strongly depends on the location of water-tube gauges inside the underground, while the amplitudes of the first-class signals are similar for all the gauges. These observations clearly indicate the atmospheric origin of the second class of registered signals.

Keywords: interferometry, time series analysis, tides, planetary waves, acoustic-gravity waves, surface waves, free oscillations, ionosphere/atmosphere interactions

1. INTRODUCTION

The instruments that provided us with the signals of the range 10^{-3} to 10^{-4} Hz are two long water-tube (WT) tiltmeters installed in the Geodynamic Laboratory (GL) of the Space Research Center in the Sudetes Mountains, SW Poland (Kaczorowski, 2006). The main elements of these tiltmeters are two disconnected, mutually perpendicular tubes with a length of 65.24 and 93.51 m, located at azimuths –121.4° and –31.4°, respectively. The hydrodynamic systems of both WTs are isolated from the surrounding environment to protect the tubes against any deformations caused by variations in atmospheric pressure.

Low-pass dampening systems applied in the WT tiltmeters for multiple times confirmed their effectiveness of allowing to register the long periodic signals of frequencies from 10^{-3} to 10^{-4} Hz several tens of minutes after the strong seismic signals of high frequency. At the same time, WT tiltmeters provided us with correct signals without significant phase delays and significant loss of tidal amplitudes, which was confirmed by the results of tidal analysis.

At the ends of the tubes (Fig. 1), there are interferometric gauges with frequency stable He–Ne laser. A phase analysis of interference images applied in the elaboration of observations ensures accuracy of measurements of water level variations by the range of single nanometers, that is, 10^{-9} m. This precision of the WT measurements ensures the accuracy of a single microarcsecond of measurements of the plumb line variations (proportionally to the length of the tubes) and 10^{-5} Pa accuracy of the pressure vibrations (1 Pa is the pressure corresponding to 0.01 m height of water column). Registration and investigation of the signals of the range 10^{-3}–10^{-4} Hz became possible, thanks to the precision of the WT measurements.

The capability of the long WT tiltmeters for measurements of middle-high frequency signals has been confirmed in the paper published by Ferreira et al. (2006).

The issue of the signals of the range 10^{-3}–10^{-4} Hz registered by the WTs had previously been reported in Kaczorowski (2013). In that paper, the topic of strong harmonic signals of the order of 10% of the tidal wave amplitudes as registered by the WTs had been discussed. These strong signals are registered only by the gauge of the Channel No. 01 of the WTs, with the location nearest to the entrance of the underground of the GL.

The existence of an evident correlation between magnitudes of the harmonic signals and a location of the WT gauges in the underground corridors suggests that the strong signals observed in Channel No. 01 are associated with very low-frequency atmospheric infrasound (Kaczorowski, 2013; Benioff, 1939; Ponomarev, 1996), and not with the Earth solid body signals.

The harmonic signals of the atmosphere pressure microvibrations affect the water level in tiltmeter tubes by the inverse barometric effect (Posmentier, 1967). The inverse barometric effect is well known in the literature, in particular, for seas and oceans. When high atmospheric pressure (created over the land surface) appears at the sea border, the level of the sea decreases and inversely, when there is a low pressure, the sea level increases. This process ensures that it fulfills the equilibrium between the pressure of water pillar and the air pressure. Similar effect of air pressure compensation occurs in the WT tiltmeters.

Pressure microvibration signals are registered by the WTs similarly as highly sensitive microbaroms (Kaczorowski, 2013).

The signals of the free Earth oscillations, produced by very strong earthquakes, as well as signals of the atmosphere pressure microvibrations interfere with each other inside the instruments (WTs). Signals of the free Earth oscillations cause activation of WT through the lithosphere, while infrasound signals activate WT by the atmospheric medium.

The origin of the pressure microvibrations has not been recognized yet; nevertheless, some properties of this phenomenon have been determined.

In this paper, we present observations registered in selected periods between the years 2004 and 2012, in which two extremely large earthquakes occurred, namely, the Sumatra–Andaman earthquake on December 26, 2004 and the Japanese earthquake on March 11, 2011.

Data series from several weeks before and after the aforementioned earthquakes had been selected to determine the impact of the earthquakes on amplitudes of the Earth's vibrations.

In the signals from Channel No. 01 of the WTs, we have observed several events presenting the effects of interaction between the signals of low-frequency atmospheric pressure microvibrations and the signals of the free Earth's oscillations.

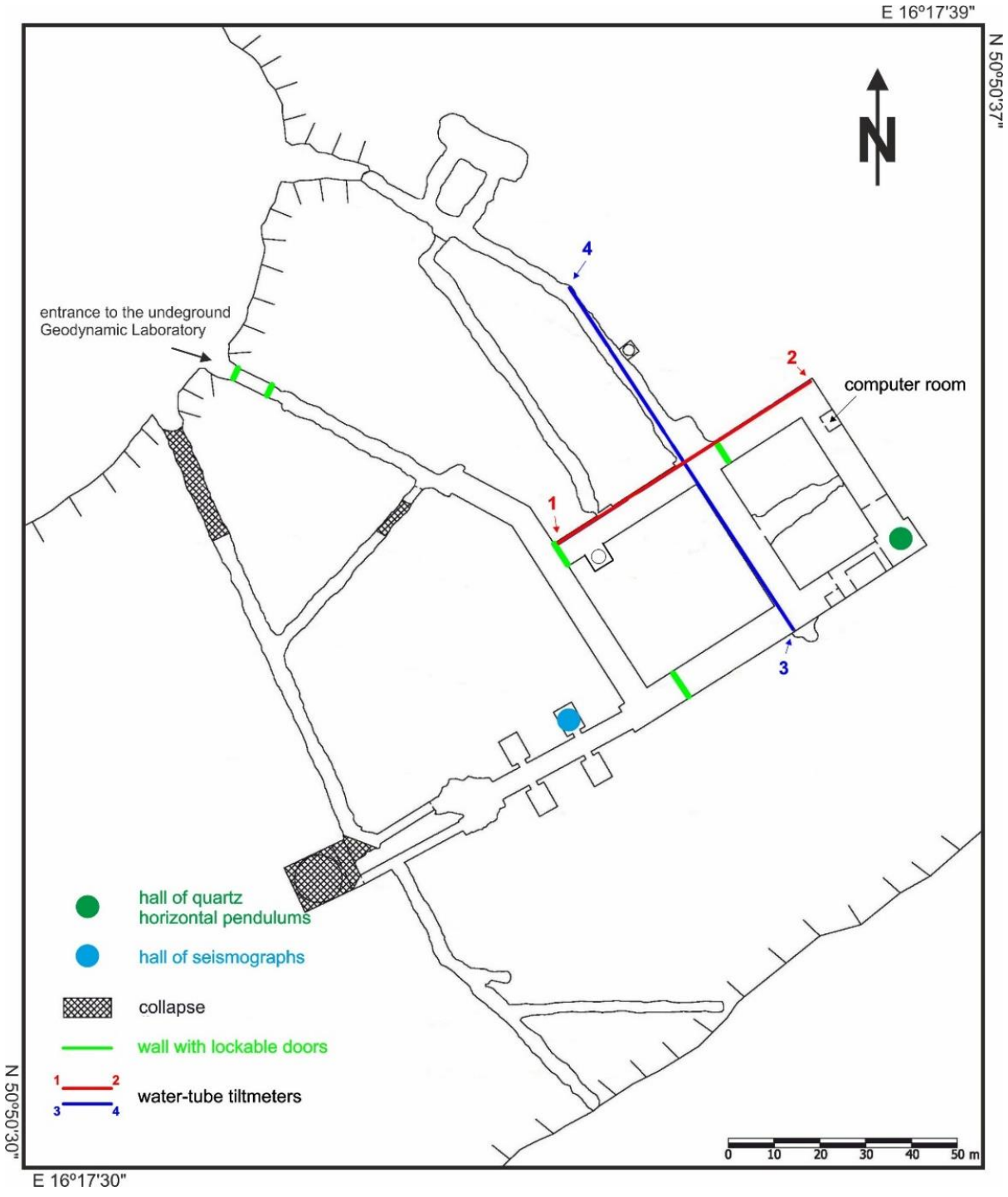

Figure 1. Plan of the underground of the Geodynamic Laboratory in Książ

2. SOME ELEMENTS OF CONSTRUCTION AND PRINCIPLES OF THE MEASUREMENT SYSTEM OF THE WT TILTMETERS IN THE KSIĄŻ LABORATORY

Discussed in this paper are the signals consisting of two components. The first component of these signals is formed of post-seismic Earth's solid-body free oscillations observed in all the

channels of instruments with similar amplitudes. These signals are one-and-a-half order weaker than the second component signals, that is, atmospheric pressure microvibrations registered in Channel No. 01 (see Section 4) (Kaczorowski, 2006; Tanimoto, 2011).

The second component of the signals consists of atmospheric pressure microvibrations. Pressure microvibrations in the range 10^{-3}–10^{-4} Hz and of the order of 10^{-3} Pa cause changes in the water level WT hydrodynamic systems of the order of 300–500 nm, which is 100 times greater than the accuracy of the WT single measurements (Kaczorowski, 2013). The second-class signals as well as the first-class signals belong to the same range of frequency, that is, 10^{-3}–10^{-4} Hz. This circumstance hinders the simple separation of the superposed signals of both classes, which are registered by the WTs.

To improve the separation of the signals of the range 10^{-3}–10^{-4} Hz from other signals, the previously applied method had been modified (Kaczorowski, 2013). On the basis of long-lasting measurements, we obtained precise tidal ephemeris, which was applied to the model of the tidal effects within the hydrodynamic system of the WTs (Ozawa, 1967).

The modeled signals had been supplemented with the trend of water evaporation to construct a more realistic model for the reduction of our observations. In the next step, we subtracted from the observations the tidal ephemeris signals with a linear trend. After that, a 120-min sampling spline of the second-order polynomial with a 1-min sampling interval had been performed, representing the long periodic or systematic trend. After the reduction of a 120-min sampling spline, we had obtained the remaining signals containing the high-frequency signals and the signals of the range 10^{-3}–10^{-4} Hz. In order to reduce the high-frequency signals, we had applied N60S5M01 filter, which belongs to ETERNA package (Wenzel, 1996).

WT tiltmeters belong to the group of tidal instruments that measure the angular variations of the plumb line. Instrument is rigidly connected to the ground – solid rock foundation. The angular variations of the plumb line are measured in relation to this foundation (Fig. 2). The WT tiltmeters measure plumb line variations with a tidal accuracy, that is, single milliarcseconds or height (Kaczorowski, 2004).

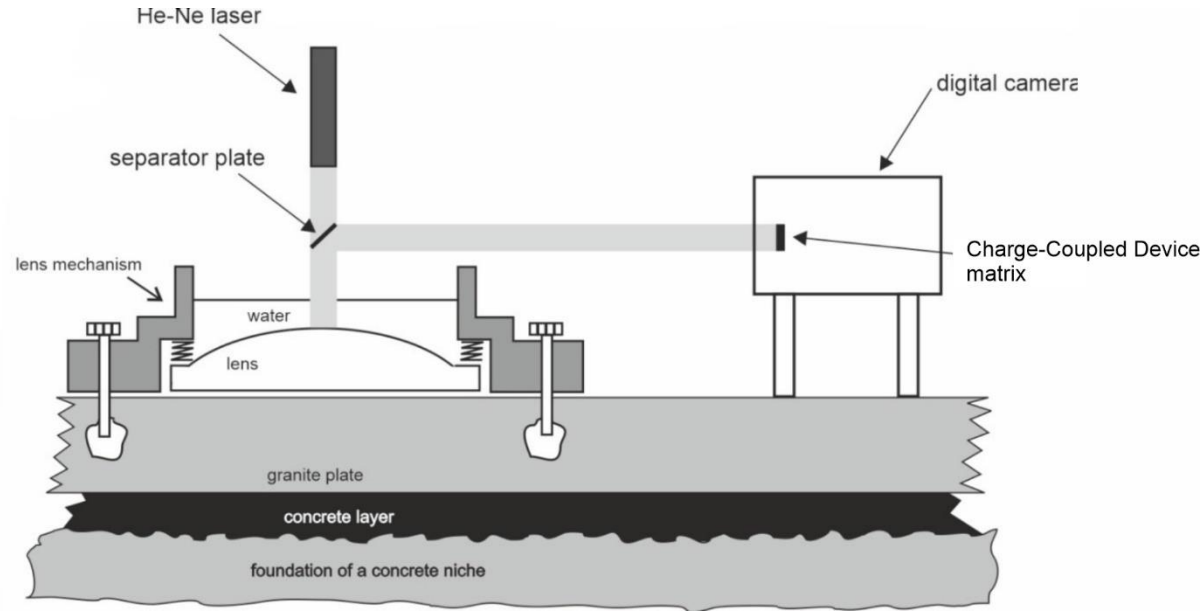

Figure 2. Block diagram of the water-tube tiltmeter measure platform

Classic Newton interference measuring devices (interferometers) had been used to measure changes in the water level in the WTs. For the refractive index of distilled water $n \approx 1.3$ and

wavelength $\lambda = 6.72 \cdot 10^{-5}$ of the red laser light He–Ne, the value of the quotient is $\lambda/2n = 2.58 \cdot 10^{-5}$ cm. Assuming that the distance between the adjacent Newton rings is measured with a relative accuracy of at least 10%, the accuracy of water level changes in classic Newtonian interferometers is not more than $0.1 \cdot (\lambda/2n) = 2.58 \cdot 10^{-6}$ cm.

Thus, at the ends of the longer water tube, that is, 93.51 m, change in the water level produced by a tidal wave with an amplitude of 15 mas (the mean value of the amplitude of the tidal wave M2 for the average latitudes of Poland) is $3.6 \cdot 10^{-4}$ cm. Therefore, for a Newtonian interferometer, the relative error of a single measurement of the signal produced by the wave M2 is $1.258527 \cdot 10^{-2}$. These accuracies are confirmed by the results of a tidal analysis, for example, the Root-mean-square (RMS) error of M2 wave equals to 0.315 mas and the result of the adjustment of the series of plumb line variations data from a long WT tiltmeter shows that the RMS error is 0.5642 mas.

Construction of the WT hydrodynamic system preserves the free surface of water lengthwise in the tubes. The tubes are only partially filled with water, which ensures minimization of an instrumental drift caused by the temperature variations. Furthermore, the impact of the temperature variations in the underground of the Książ GL is relatively small and does not exceed 0.1°C in a year.

The hydrodynamic systems of the WTs had been equipped with dampening elements to protect the instruments against the effect of resonance, that is, water waving effect after strong seismic events.

Applied in the WTs, the dampening filters consist of barriers (Fig. 2) that transversely divide the instrument tubes. Barriers are placed with a spacing of around 4 m along the entire length of the tubes. The flow of water between the sections takes place only through holes of approx. 1.5 mm in diameter. The diameter of the holes was selected empirically through many tests.

An additional 1-mm-diameter hole had been made above the water level in each section (Fig. 3). These openings ensure the atmospheric pressure is in balance with the pressure inside the pipe. Thanks to this solution, air movements produced by the pressure changes take place in the space outside the pipe. For obvious reasons, systematic air movements inside the pipe, which could disturb the free surface of the water, do not occur. Due to lack of systematic air movements, the condition of free surface of the water inside the tube is fulfilled in the whole length of the pipe. Therefore, we are able to interpret the level of water inside the pipe as quasi-equipotential surface. This is a very important circumstance which enables us to investigate tidal phenomena (Kaczorowski, 2005).

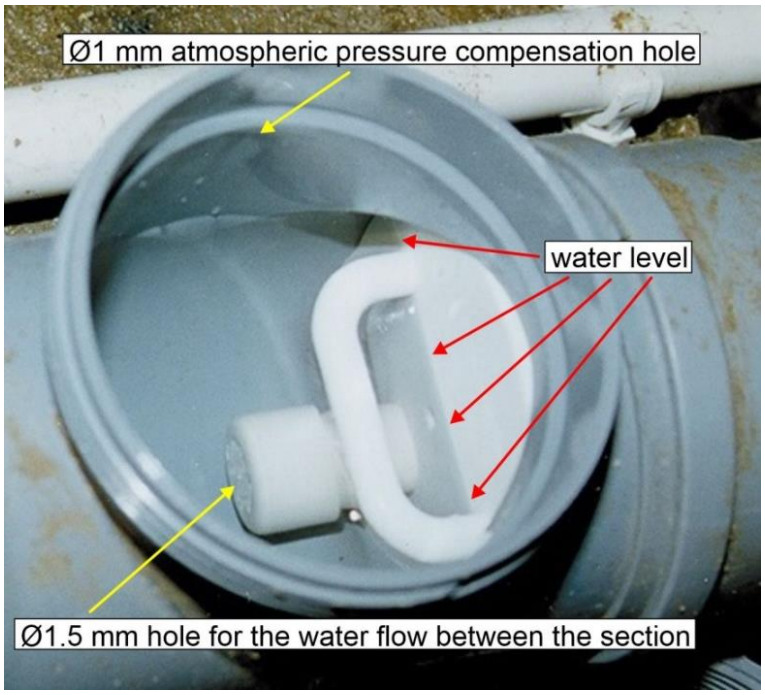

Figure 3. View of the elements of a barrier section of the water-tube tiltmeter pipe

The earthquakes waves, Earth's free oscillations, or any other phenomenon may cause a waving effect only in the space of 4-m-long sections of tiltmeter pipes. To the next section/sections of the pipe, the waves' undulations penetrate only through the 1.5-mm-diameter hole in the separating barriers (Fig. 3).

After several minutes from the inertial or gravitational–inertial moment of the impulse (e.g., the acceleration of a seismic wave or the Earth's free vibrations), the oscillations of water in the subsequent sections of the pipe meet in different phases, and thus very strongly dampen one another.

The damping capability of the system shows the following example. If we add 1 dm^3 of water to the first section of the WT pipe, the signal would appear in the last section of the WT pipe after more than 8 min – changes observed in the interference images. The return signal after reflection of the wave in the measuring station of the first pipe section is completely damped. At the same time, the described system represents a large inertia in response to geodynamic signals.

The dampening system has proven to be effective after strong earthquakes and allows registering the long periodic signals of frequencies from 3×10^{-3} to 10^{-4} Hz. Such registering was possible several tens of minutes after the high-frequency strong seismic signals. This confirmed that the water waving dampening system applied in the WTs presents a time constant of several hundred seconds in length.

The correctness of the WT dampening system had also been documented in tidal measurements. Results of the tidal analysis showed a lack of delay effect of the phases of tidal signals caused by instrumental reasons as well as the effect of decrease in the amplitudes of tidal waves (Kaczorowski, 2004, 2005, 2006).

3. MACQUARTE ISLAND AND NORTHERN SUMATRA EARTHQUAKES ON DECEMBER 23 AND 26, 2004

In December 2004, two extremely large earthquakes took place: the first one in the north of the Macquarte Island on December 23 with a magnitude of 8.1, and 3 days later, the second one off the west coast of the northern Sumatra on December 26 with a magnitude of 9.0.

The time periods of observations before and after the large earthquakes offer a good opportunity to investigate the impact of an earthquake on the signals of the range 10^{-3}–10^{-4} Hz. Two-week-long plots of the signals registered in the time period of the large earthquakes by four gauges of the WTs are presented in Figs 4–7.

In the time period preceding these strong earthquakes, the average amplitudes of the signals of the range 10^{-3}–10^{-4} Hz were different in the different channels of the WTs (Fig. 4). The greatest oscillations were observed in Channel No. 01, where their amplitudes varied in the range of –0.15 to 0.15 μrad (Fig. 4). In the other channels, the signals were one order weaker. After the strong earthquakes, the mean level of the signals of the range 10^{-3}–10^{-4} Hz did not change radically for all the channels (compare left sides with right sides of the plots in Figs 4–7) and proportions between the magnitudes of the oscillations had been conserved in these channels.

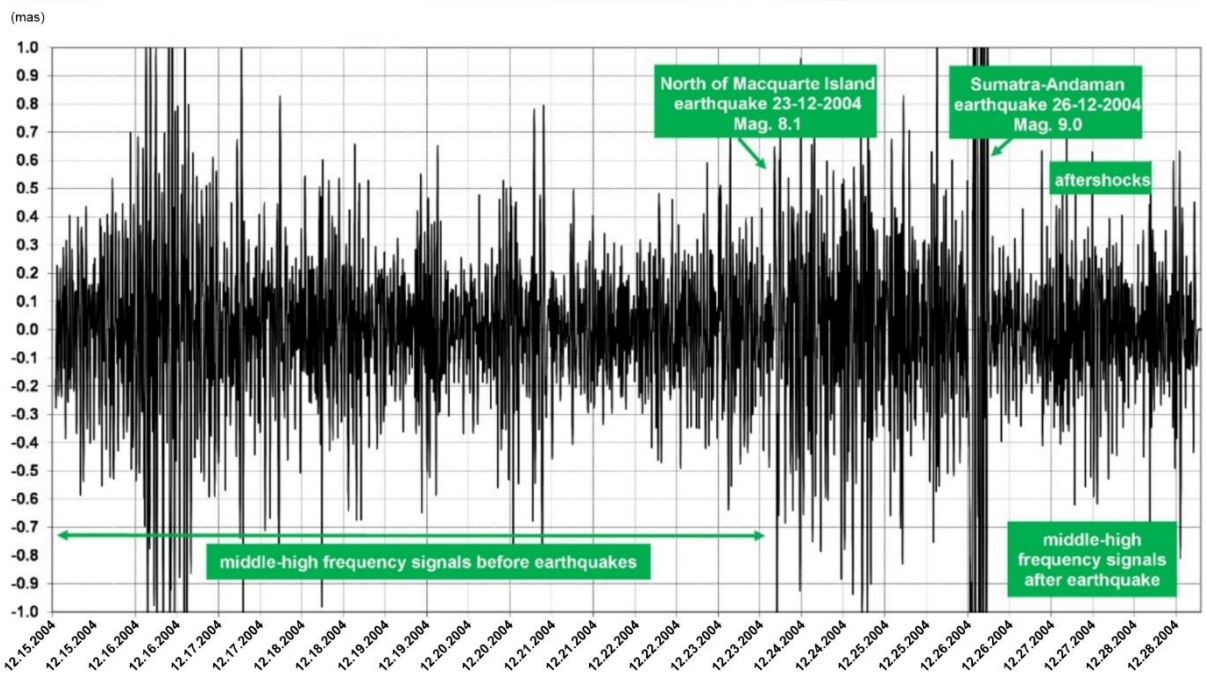

Figure 4. The plot of 2-week-long signals of the range 10^{-3}–10^{-4} Hz in the time period from December 15 to December 28, 2004 in Channel No. 1

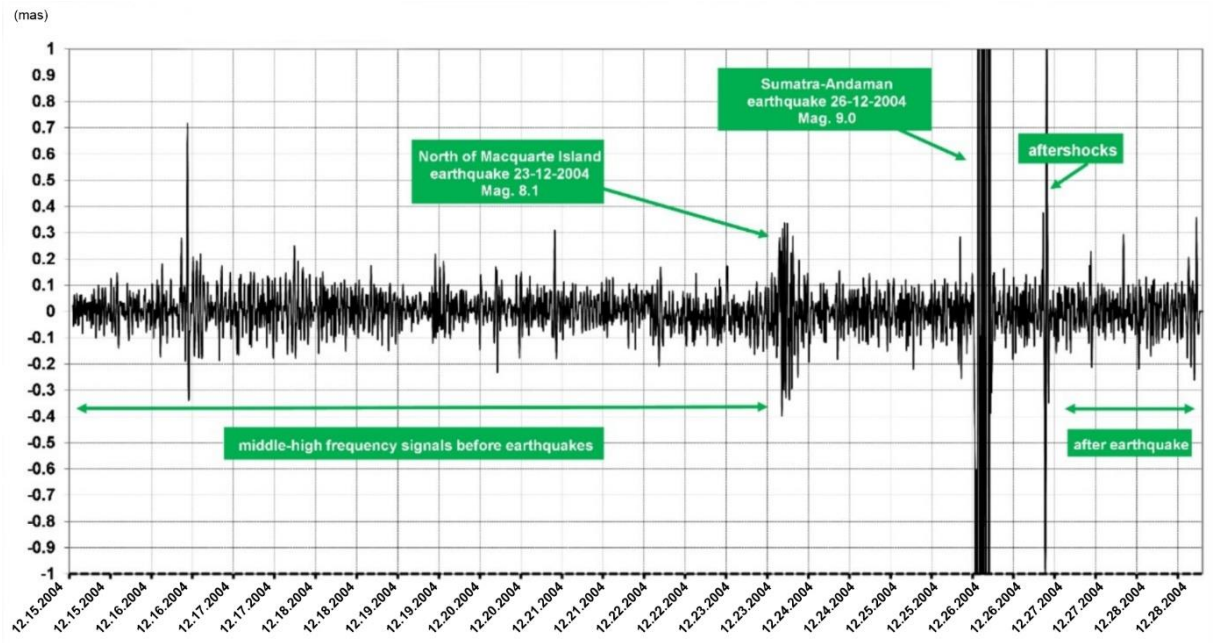

Figure 5. The plot of 2-week-long signals of the range 10^{-3}–10^{-4} Hz in the time period from December 15 to December 28, 2004 in Channel No. 2

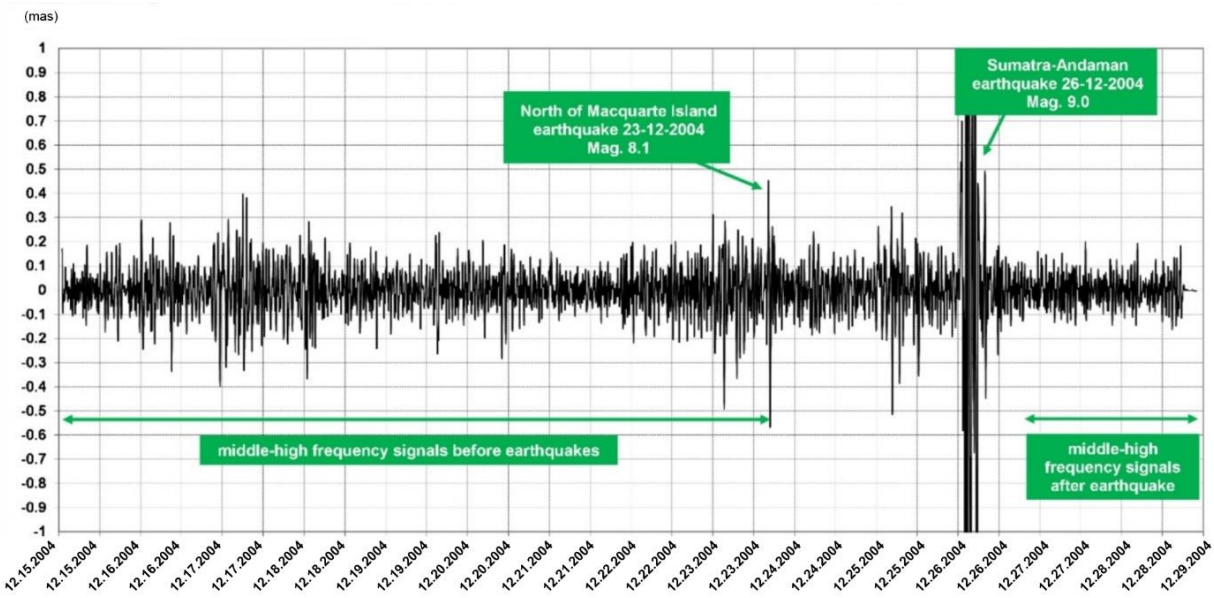

Figure 6. The plot of 2-week-long signals of the range 10^{-3}–10^{-4} Hz in the time period from December 15 to December 28, 2004 in Channel No. 3

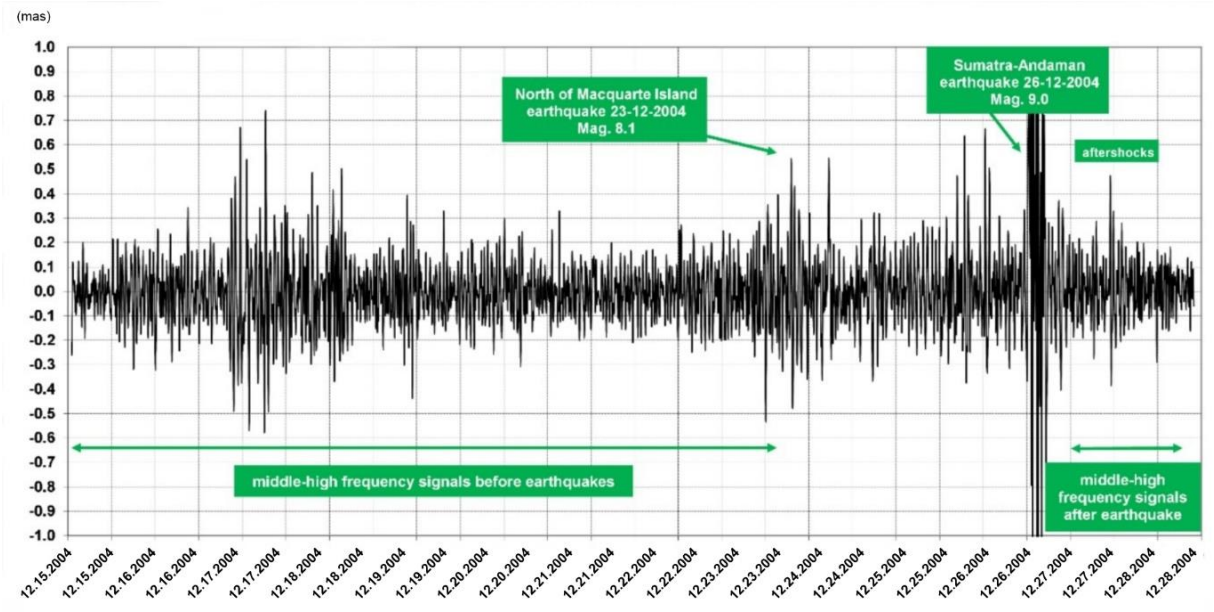

Figure 7. The plot of 2-week-long signals of the range 10^{-3}–10^{-4} Hz in the time period from December 15 to December 28, 2004 in Channel No. 4

Detailed plots of the signals of the range 10^{-3}–10^{-4} Hz observed in Channel No. 03 before, during, and after the earthquakes are shown in Fig. 1S, plots B–E. It was observed that the signals were destroyed by the earthquake within ca. 5 h only and afterward, they revived (plots C and D). One day after the Sumatra earthquake, the signals returned to their previous magnitudes (plots B and C). The process of disappearance of the signals is shown on plots E and D. The appearance of seismic waves P and S deformed the signals of the range 10^{-3}–10^{-4} Hz (plot E), and then, the strong surface waves destroyed them fully (see the central part of the plot D).

Subsequently, we proceeded with 227 analyses of the data series, which had been performed in the same manner, that is, Fourier analysis of 4-day-long data windows and a 1-h-long step.

Plot B in Fig. 8 consists of overlap of 40 spectral analyses obtained based on the 1-week-long data series from before the earthquake in the north of the Macquarte Island (December 23, 2004). The results of the Fourier analyses confirm that the signals of the range 10^{-3}–10^{-4} Hz before the earthquake in the north of the Macquarte Island were of a harmonic character; nevertheless, some of the determined modes were not in accordance with the theoretical modes of the Earth's free vibrations (first class of signals; plot B, Fig. 8) (Tanimoto, 2011).

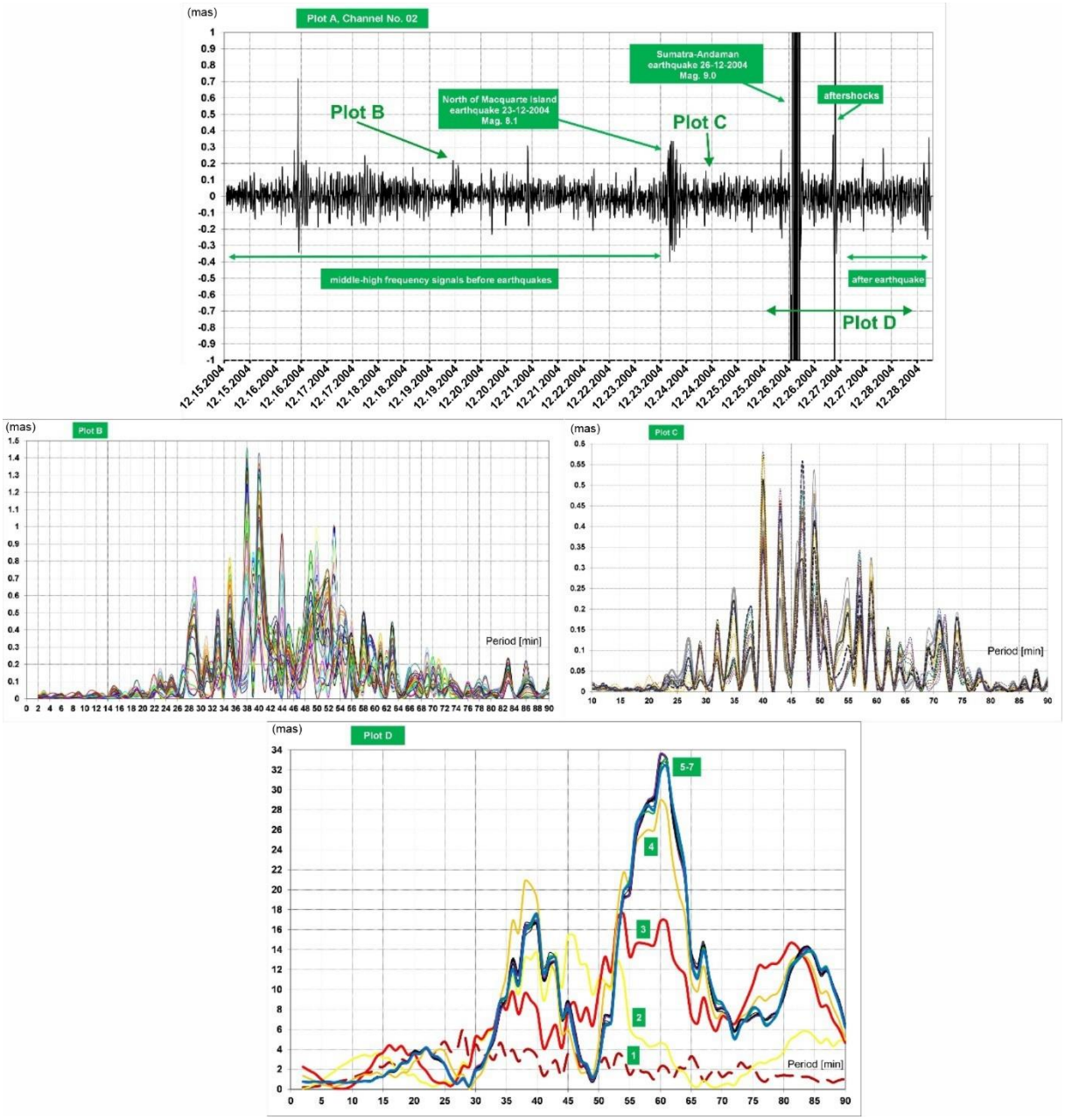

Figure 8. Results of the Fourier analyses of the signals of the period ranging 10–100 min in the data period from December 15 to 28, 2004, as registered in Channel No. 02

The results presented on plot C (Fig. 8) show that after the Macquarte earthquake and before the Sumatra earthquake at the same time, new frequency modes had appeared, while some existing modes had been reduced (Rhie, 2004).

The results of data analyses from the interval including the main phase of the Sumatra earthquake are presented on plot D (Fig. 8). Numbers 1–7 marked in Fig. 8 denote successive plots of the analyses obtained with a 1-h-long step. We observed a systematic increase in amplitudes and stabilization of their maximums for a period close to 60 min (around the fundamental mode of free oscillation). Fig. 9 shows the variability of the amplitudes of signals of the range 10^{-3}–10^{-4} Hz in the period of December 15–28 in Channel No. 02. All the plots in Fig. 9 had been obtained with 1-h-long step and periods in the range of 36–44 min. In plot A (Fig. 9), variations in amplitudes for the whole period before and during the earthquakes, as well as a large jump of amplitudes during a seismic event are shown. Detailed information on

the variability of the amplitudes is presented in plots B and C (Fig. 9). Supplementary information about variability of amplitudes of the signals in the period range 10-100 min in Channel No. 02 in the time periods of 53-58 min in December 2004 was presented in Fig. 2S.

In Channel No. 02 and Channel No. 03 (Figs 3S and 4S, respectively), we had observed variations in amplitudes with displacements of the analyzed window. Plot B (Fig. 4S) contains the results of the data analysis from the interval including the main phase of the Sumatra earthquake – there are marked numbers of series of the successive analyses obtained for a 1-h-long step of the analyzed window.

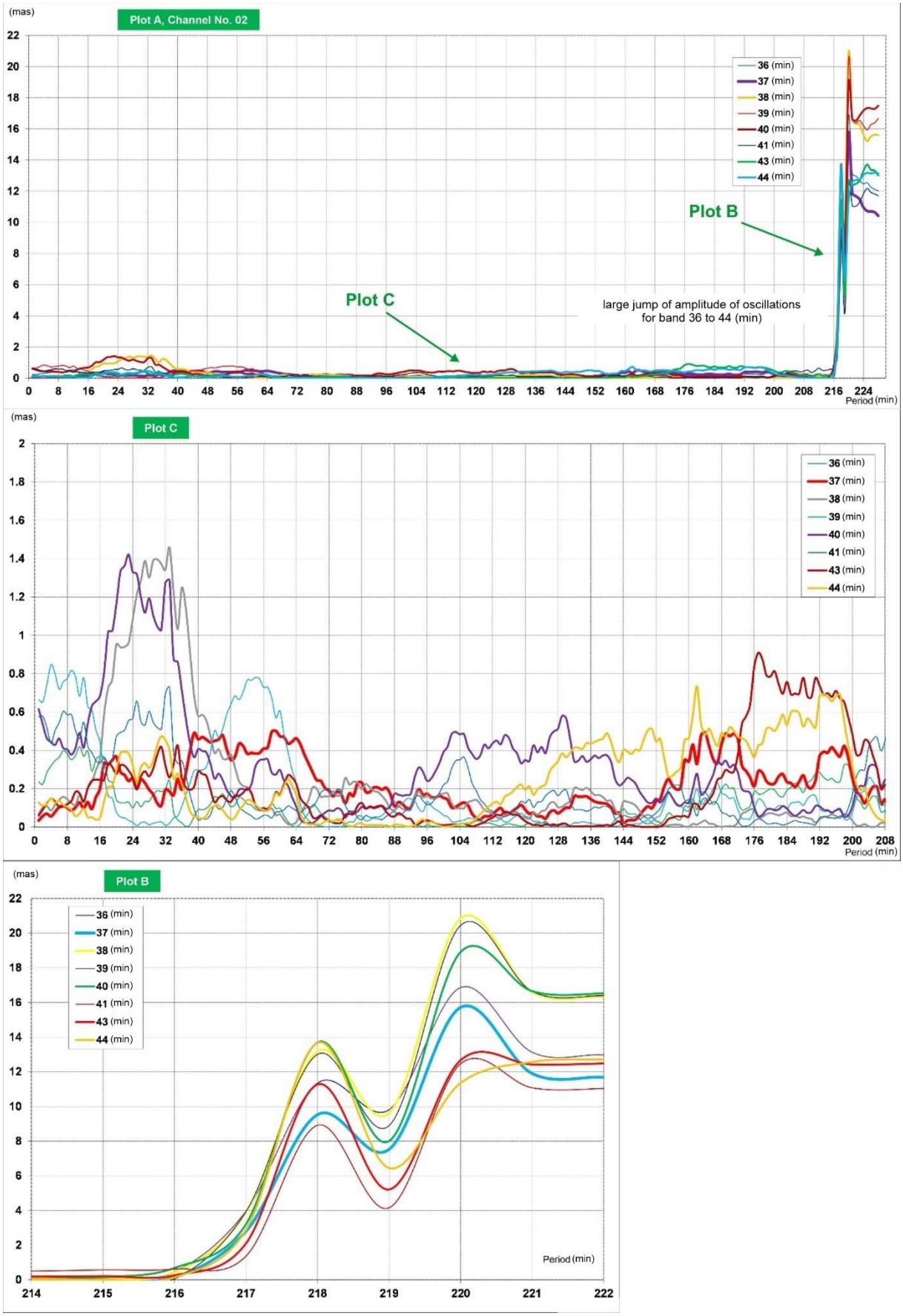

Figure 9. Variability of amplitudes of signals of the period range 10–100 min in the period of December 15–28 in Channel No. 02

4. THE JAPANESE EARTHQUAKE OF MARCH 11, 2011

On March 11, 2011, on the convergent plate boundary in the subduction zone located near the coast of Honshu (Japan), an extremely strong earthquake (Mag. 9.0) occurred.

In March 2011, signals of the range 10^{-3}–10^{-4} Hz were registered in all of the WT channels (Fig. 10, Figs 5S–7S).

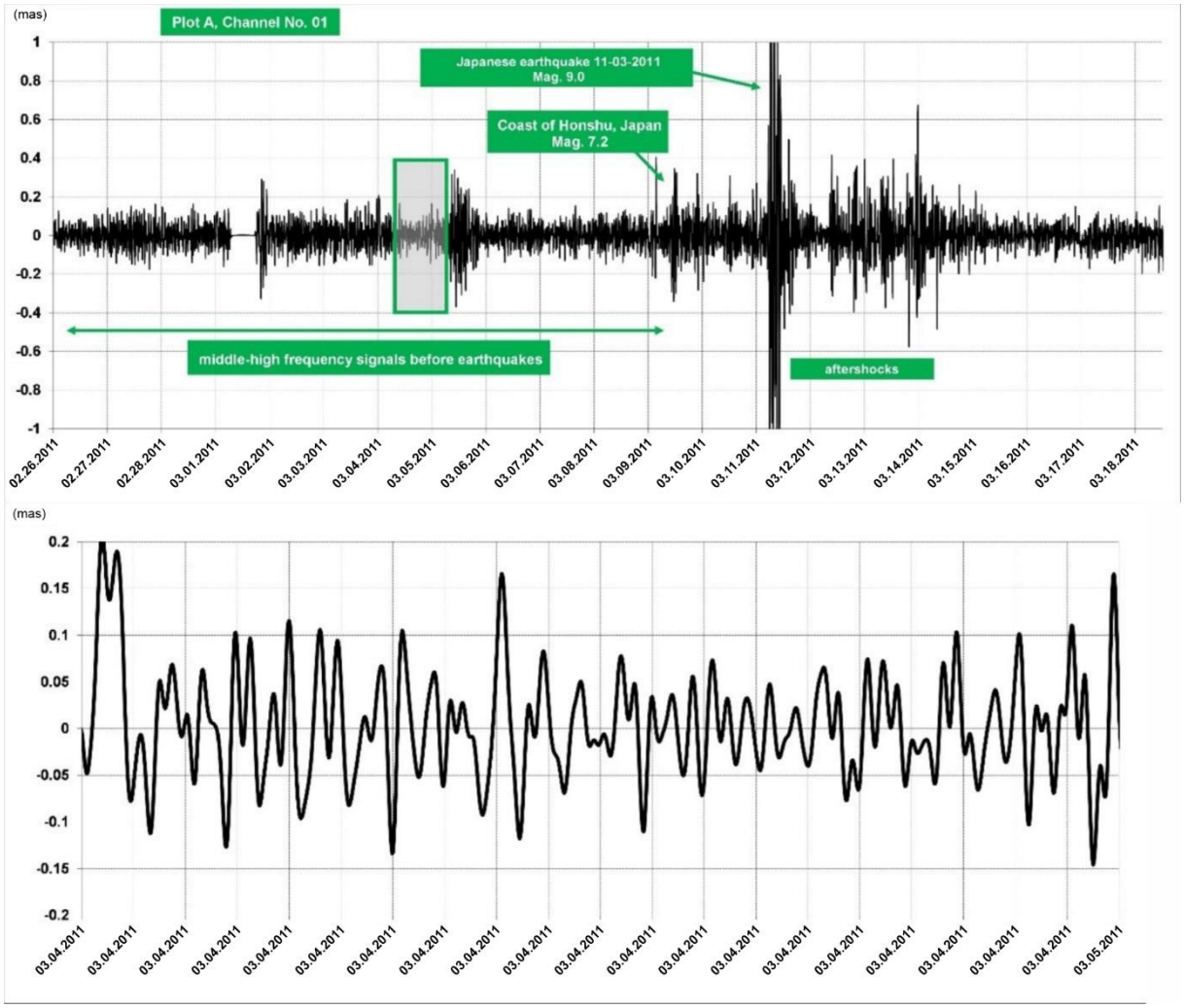

Figure 10. Signal of the range 10^{-3}–10^{-4} Hz registered by the WTs in Channel No. 01 in March 2011

The results of spectral analyses of signals in the period from February 26 to March 16, 2011, registered in Channel No. 04 of WT, are shown in Fig. 11. As in the previous analyses, we applied the 4-day-long data windows and the 1-h-long step. Plot B in Fig. 11 presents the overlap of 30 results of the Fourier analyses obtained for a 1-week-long data series before the earthquake in Honshu (Japan) on March 11, 2011.

The Japanese earthquake had been preceded by five significant earthquakes with the magnitudes of 6.5–7.2, which occurred during the period of 5 days before the huge Japanese event. Probably, these earthquakes were the reasons of the Earth's free oscillation signals observed before the huge Japanese earthquake (plot B in Fig. 11).

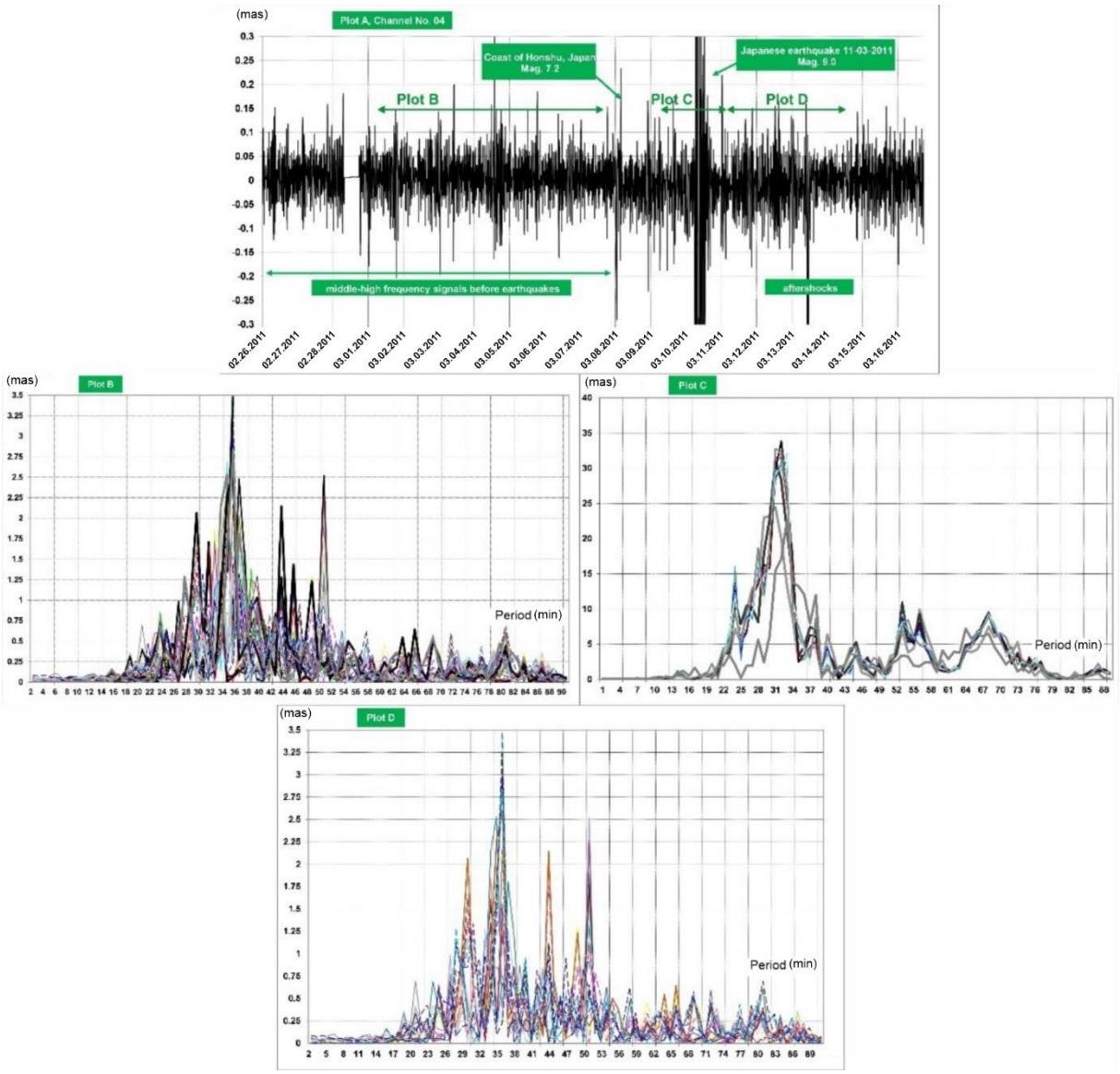

Figure 11. Results of the Fourier analyses of signals in the period range 10–100 min in the period from February 26 to March 16, 2011, registered in the WT Channel No. 04

The results of the Fourier analyses confirm the harmonic characteristics of the Earth's free oscillations and atmospheric pressure microvibration signals. Probably, due to interference between both classes of signals, results of spectrum analyses only partially agree with the spectrum of modeled free vibrations of the solid Earth (plot B in Fig. 11 and plot B in Fig. 8).

Plot C (Fig. 11) was obtained with the same method as plot D (Fig. 8) during the main phase of the Honshu earthquake (Japan). Relocation of the analyzed window by 4-h-long interval through the main phase of the Japanese earthquake shows systematic increase of the amplitude of oscillations and stabilization of its maximum for the period close to 31 min (see plot C, Fig. 11). In the case of Sumatra event, the maximum of oscillations had been reached for a period of 60 min (see plot D, Fig. 8).

Probably, the difference between the frequencies of oscillations (close to 30 min) at the moment of maximum of oscillations results from the large difference between the size of epicenters of both earthquakes. In the Northern Sumatra earthquake, it was about 1400 km (Lay et al., 2005) and for the Honshu earthquake (Amici et al., 2013), it was 250 km only.

The development of the signals in the range 10^{-3}–10^{-4} Hz about 3 days and later after the main phase of the Japanese earthquake and partially the aftershock is shown in plot D (Fig. 11). Plot D (Fig. 11) consists of an overlap of 64 spectral analyses obtained based on the about 1-week-long epoch of observations.

The results of the Fourier analyses confirm that the signals after the Japanese earthquake possess harmonic characteristic, which is in accordance with the theoretical modes of the Earth's free vibrations (first class of signals; plot D, Fig. 11) (Tanimoto, 2001). This accordance is better visible for plot D than for plot B from before the main earthquake (Fig. 11).

In Fig. 12, the average amplitudes of the signals of the range of 10–3–10–4 Hz are shown in functions of periodicity from the surroundings of the Japanese earthquake. The plots had been prepared on the basis of results of the spectral analysis of measurements from Channel No. 04 of the WTs.

The average amplitude function from the time period before the Japanese earthquake had been compiled on the basis of 71 analyses, whereas after the earthquake, the mean amplitude function had been determined on the basis of just 26 analyses.

After the earthquake, the plot of average amplitudes showed an increase of amplitudes of the high-frequency modes (see the left side of Fig. 12) for a maximum 34-min period.

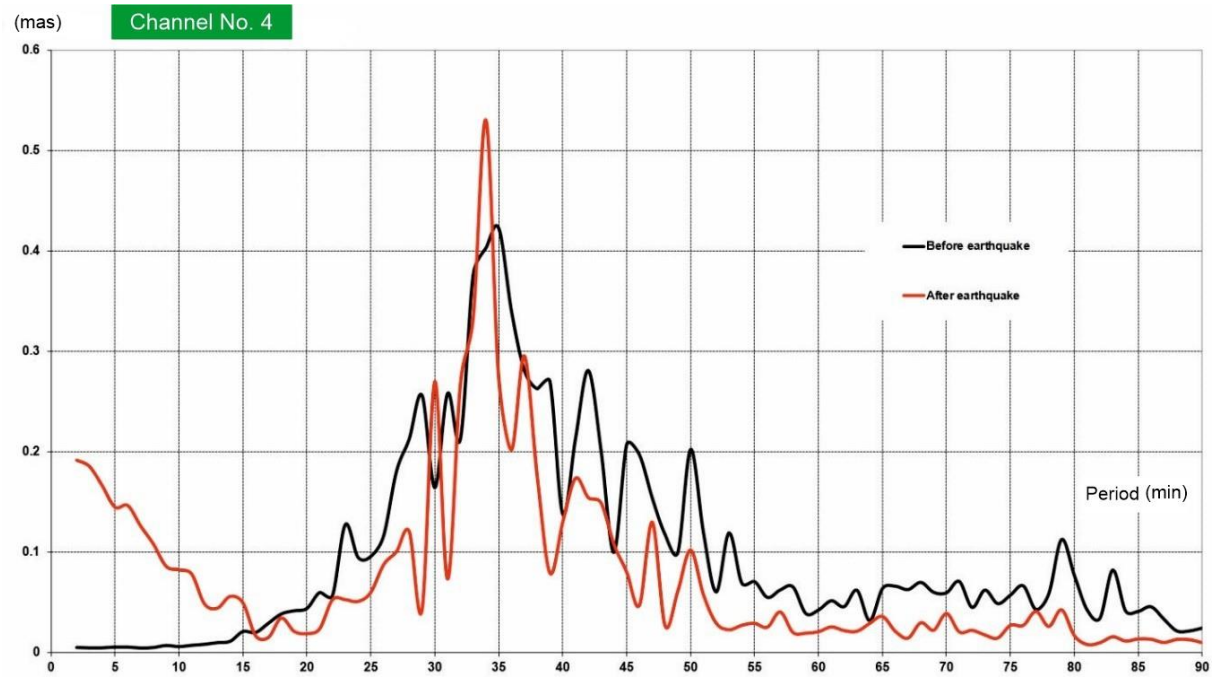

Figure 12. Plots of the average amplitude function of the signals of the period range 10–100 min from before and after the Japanese earthquake

5. LOW-FREQUENCY ATMOSPHERIC MICROVIBRATIONS – THE SECOND-CLASS SIGNALS

The atmospheric pressure microvibrations are the second component of the family of signals of the range 10^{-3}–10^{-4} Hz registered by the WTs (Kaczorowski, 2013; Tanimoto, 1999, 2001).

The mechanism of transfer of the signals of atmosphere pressure microvibrations to the hydrodynamic system of the WTs is the inverse barometric effect. In the presented discussion, the atmospheric pressure signals were recalculated from micropascal units to angular units, that is, milliarcseconds.

This recalculation of units is useful for comparison of signals of the Earth's free oscillations and signals of atmospheric pressure microvibrations.

The sensitivity of interference gauges of WT is close to the single nanometers. This sensitivity corresponds to 10^{-5} Pa of pressure variations (Kaczorowski, 2006). Therefore, the WTs are at the same time microbarometers, which are able to register the air pressure microvibrations of magnitude until 10^{-5} Pa (Posmentier, 1967). The atmospheric pressure signals had been observed on Channel No. 01 in two modes of large and small amplitudes. Amplitudes of strong air pressure microvibrations are close to 0.5 mas, and amplitudes of low microvibrations are close to 0.15 mas (Fig. 13).

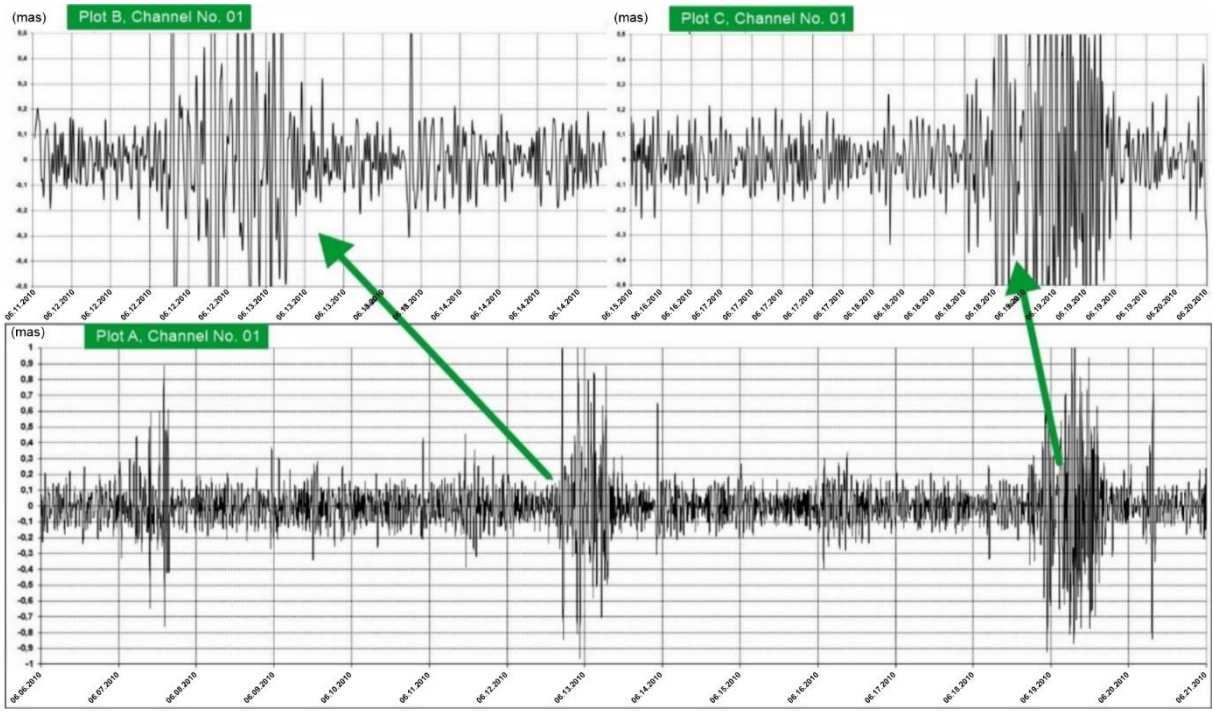

Figure 13. Small and large amplitude signals of the atmospheric microvibrations observed in Channel No. 01 in the period from June 6 to 21, 2010

From June 6 to 21, 2010, single-day-long events of strong signals were observed on Channel No. 01 irregularly, while the weak signals existed on Channel No. 01 almost permanently (Fig. 13). The strong signals of the atmospheric pressure microvibrations never appeared on the other channels of the WTs. Large and small amplitudes of the atmospheric microvibrations were observed in 2012 on Channel No. 01 (plot A on Fig. 14). In that year there was registered three weeks long event of strong signals (from February to March, 2012; Fig. 14).

The results of spectral analyses of the weak amplitude signals from the epoch preceding long epoch of strong signals in 2012 (plot A in Fig. 14) are shown on plots B–D in Fig. 14.

The plots B and C in Fig. 14 possess three outstanding peaks close to 6 mas magnitude and 28, 36, and 40 min periods. The peaks increased with periodicity until 40 min. Very similar plots of spectral analyses were obtained for weak amplitudes of harmonic signals from 2010. From June 18 to 20, 2010, the plots of spectral analyses also composed of free outstanding peaks and amplitudes closed to 7 mas for weak microvibrations. The periods of peaks are 23, 25, and 28 min in the period from June 18 to 20, 2010 (Fig. 15). During short periods of strong atmospheric microvibrations (Fig. 13), the amplitudes of resonances increase to 40 mas (Fig. 15B).

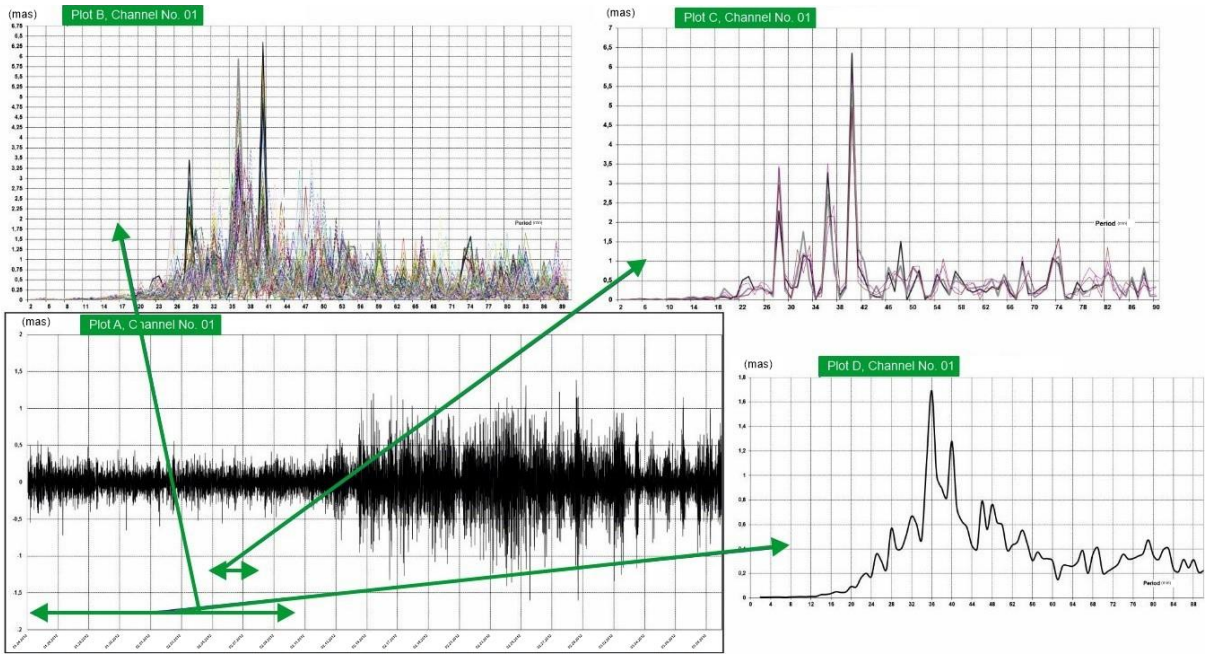

Figure 14. The epochs of observations which contain signals of large and small amplitudes of the atmospheric microvibrations and results of spectral analyses of signals from the epoch preceding period of strong atmospheric microvibrations in March 2012 on Channel No. 01 (plot A)

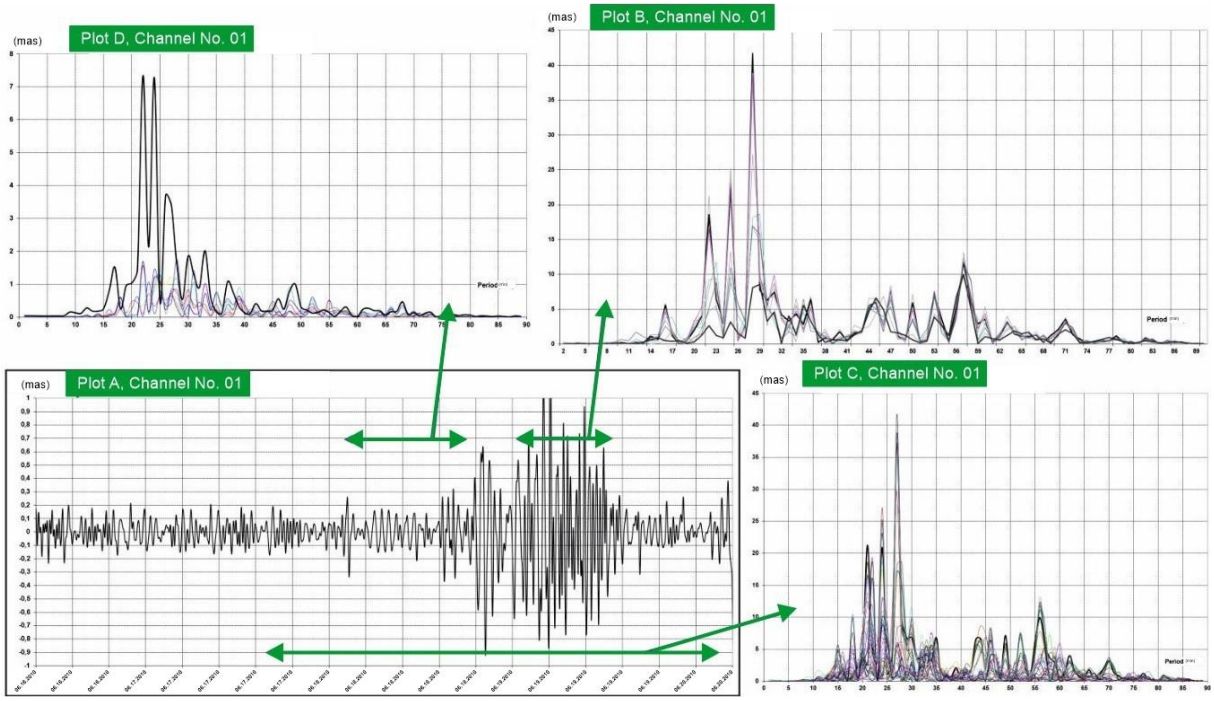

Figure 15. The results of spectral analyses for weak and strong signals from June 18 to 20, 2010

The results of spectral analyses of strong signals observed on Channel No. 01 in the period from February 2 to March 3, 2012 are shown on plots B–D of Fig. 16.

The plot of spectral analyses of strong signals appeared to be quite different from the spectrum of weak amplitude signals. In strong signals spectrum, there are no clearly distinguished peaks, as in the case of weak signals. During a long-lasting event, the strong magnitude peaks reach 30 mas (Fig. 16A).

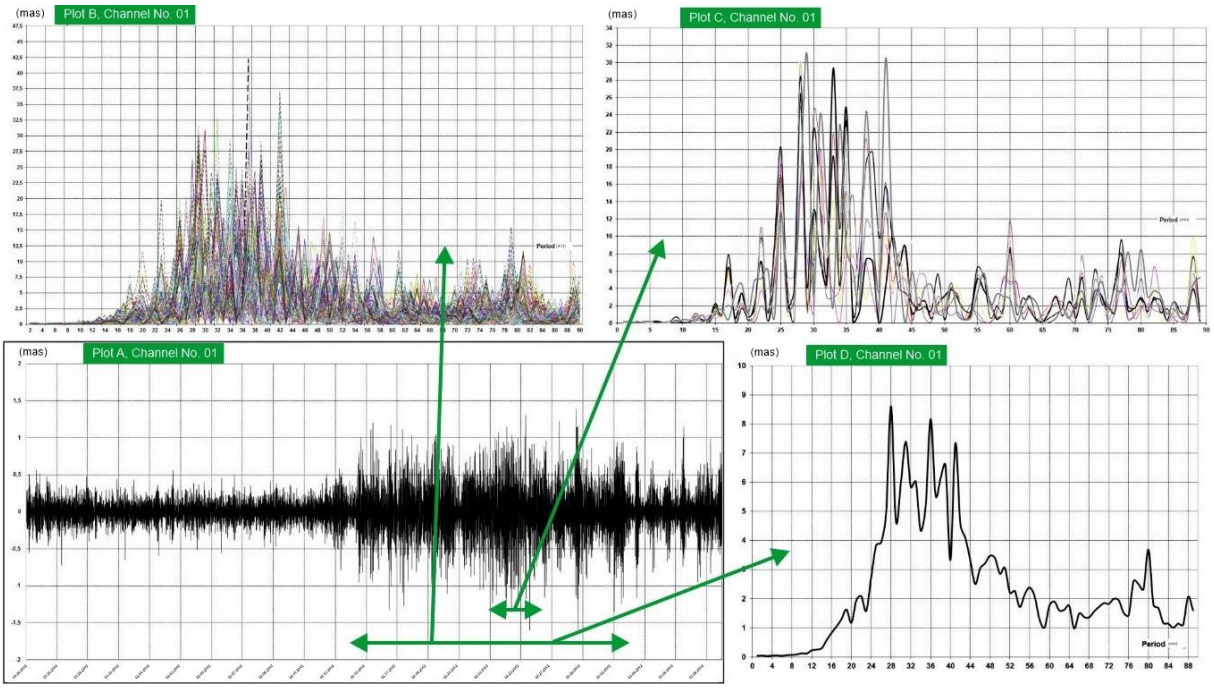

Figure 16. Overlapped results of 80 spectral analyses of 3-week-long data series in the epoch of strong infrasound signals in the period from February 2 to March 3, 2012

In plot A of Fig. 16, there is visible large variability of signals, which reflects in the form of muddied shape of spectral modes (Fig. 16B). In plots B and C of Fig. 16, dozen peaks reach 30 mas. The peaks overlap each other, which indicates the complexity of signals. This situation strongly contrasts with regular and repeating plots of spectral signals for weak signals of the atmospheric microvibrations (Figs 14B and 15B, C).
The similarities between the results of Fourier analysis of the weak signals registered in 2010 (Fig. 15B, C) and 2012 (Fig. 14B) suggest existence of the resonant effect.

In both plots, dominant modes possess similar shape of Fourier spectrum, similar periodicity and magnitudes. The similarities of Fourier spectrum of the weak signals between the 2-year-long distant epochs of observations indicate high invariability of mechanism of the resonance. No significant variations of the mechanic of resonance in the scale of the 2 years were observed.

6. CONCLUSIONS

The abilities of measurement of WTs caused extension of areas of our investigation on the middle-high frequency signals (Ferreira, 2006). The signals of the range 10^{-3}–10^{-4} Hz that are observed by WT in the Książ GL consist of two families of harmonics that are produced by two classes of phenomena.

The first class of signals is well known as the Earth's solid body free vibrations which appeared after strong earthquakes. The first class of signals affected water level in WT hydrodynamic system by kinematic as well as gravity accelerations produced by strong earthquakes in the form of gravity-seismic waves.

The signals of second class of phenomena appeared in WT hydrodynamic system through inverse barometric effect. These signals belong to the low-frequency microvibrations of atmospheric pressure, that is, very low-frequency atmospheric infrasound.

The signals of the first-class phenomena are transmitted by lithosphere and observed on all channels of the WTs independently of the location of gauge in the underground corridors.

Inversely, the second-class phenomena strongly depend on the location of gauges in the underground and its distance from the entrance.

The first-class signals of harmonic character are associated with large-scale global resonances in the space of the solid Earth. This class of signals produced by earthquakes is associated with global resonance, that is, the Earth's free vibrations.

The second class of harmonic signals registered by WTs are extremely low-frequency infrasound. Taking into account the velocity of propagation of sound in the atmosphere, that is, about 330 m/s (28, 36, and 40 min periods; see Section 5), close to 6 mas magnitude, we should expect the infrasound waves of hundreds of kilometers length.

The opportunity for registration of both classes of signals is created by two damping mechanisms, that is, the hydrodynamic damping mechanism (cf. Section 2) and the natural damping mechanism of infrasound signals, which occurred inside the space of the underground corridors.

The second damping mechanism is based on the phenomenon of convection pillars inside the underground corridors and the very heavy atmosphere in underground caused by very high humidity close to 98%. In our opinion, these factors are the reason for strong damping of low-frequency atmospheric signals at a distance of tens of meters, that is, to the opposite end of the tube. Because of these, the amplitude of low-frequency atmospheric signals is quickly decreasing with the increase of distance from the entrance to underground.

Our knowledge about convection process is based on the measurements taken with the help of very precise linear temperature gradientometer (40 thermometers).

In the case of low-frequency air pressure signals, the WT works like dipole. The infrasound signals are possible to be registered only in case of the existence of differences between the opposite ends of the WT, like in the case of dipole.

The harmonic characteristics of infrasound waves suggest the existence of a resonance phenomenon, which is the source of these signals. Such long waves can be produced only in a large space of size thousands of kilometers.

As was shown by Hoult (1969), acoustic waves in the upper atmosphere are associated with temporal and spatial variations in electron density in the ionosphere.

Also, the possibility of generating ion sound waves in the low latitude of the topside of the ionosphere was reported by Huba et al. (2000). The origin of very long seismo-acoustic waves is associated with surface waves and free oscillations produced by seismic activity of the Earth.

Post-seismic low-frequency oscillations of the Earth's surface are propagated to the atmosphere in the form of infrasound. The spectrum of seismic–acoustic waves was almost identical to the spectrum as seismic waves in the Earth solid media. This phenomenon was presented by Ponomarev (1996).

These coincidences explain the existence of strong resonance between signals of atmospheric infrasound and free oscillations of the Earth.

Observations from Channel No. 01 show that there are visible large changes in the shape of spectral modes (Fig. 16A) as well as in the spectral modes of infrasound modes (Fig. 16B). It is the effect of resonance between these strong atmospheric signals (Fig. 15B, C). The similarities of harmonics of both phenomena in frequency and magnitude aspects make interpretation of these signals difficult.

Effect of resonances of both signals is visible in the form of muddied shape of Fourier spectral of the Earth's body free oscillations (Figs 8B, C and 11B, D).

Because the Earth's solid body free vibration signals are modulated by the infrasound signals, the location of resonance peaks and its magnitudes are changing.

REFERENCES

Amici, S., Anzidei, M., Bignami, C., Brunori, C. A., Borgstrom, S., Buongiorno, F., ... & Stramondo, S. The March 11th, 2011, M 9.0 earthquake offshore Honshu Island (Japan): a synthesis of the Tohoku-Oki INGV Team research activities. *Quaderni di geofisica*, 2013.

Benioff, H.; and Gutenberg, B. Waves and currents recorded by electromagnetic barographs. *Bulletin of the American Meteorological Society*, 1939, 20.10: 421-428.

Ferreira, A. M. G.; d'Oreye, N. F.; Woodhouse, J. H.; and Zürn, W. Comparison of fluid tiltmeter data with long-period seismograms: Surface waves and Earth's free oscillations. *Journal of Geophysical Research: Solid Earth*, 2006, 111.B11.

Hoult, D. P. Acoustic waves in the ionosphere. Pennsylvania State University Scientific Report No. 339, 1969.

Huba, J. D., Joyce, G., & Fedder, J. A. Ion sound waves in the topside low latitude ionosphere. *Geophysical research letters*, *27*(19), 3181-3184, 2000.

Kaczorowski, M. Discussion on the results of analyses of yearly observations (2003) of plumb line variations from horizontal pendulums and long water-tube tiltmeters. *Acta Geodyn. Geomater.*, Vol. 2, No.3 (139), 1-7, 2005.

Kaczorowski, M. Earth free oscillations observed in plumb line variations from the 26 December 2004 Earthquake. *Acta Geodynamica et Geomaterialia*, 2006, 3.3: 79.

Kaczorowski, M. High-resolution wide-range tiltmeter: Observations of Earth free oscillations excited by the 26 December 2004 Sumatra–Andaman earthquake. In *Earthquake Source Asymmetry, Structural Media and Rotation Effects*; Springer: Berlin/Heidelberg, Germany, 2006; pp. 493−520.

Kaczorowski, M. Unrecognized origin signals disturbing water-tubes tiltmeters measurements in geodynamic laboratory of SRC in Ksiaz. *Acta Geodynamica et Geomaterialia*, 2013, 10.3: 171.

Kaczorowski, M. Water Tube Tiltmeter in Low Silesian Geophysical Observatory. Results of adjustment of half yearly series of plumb line variations. *Acta Geodyn. Geomater.*, 2004 Vol. 1, No.3 (135) pp. 155-159.

Lay, T., Kanamori, H., Ammon, C. J., Nettles, M., Ward, S. N., Aster, R. C., ... & Sipkin, S. The great Sumatra-Andaman earthquake of 26 december 2004. *Science*, 2005, 308(5725), 1127-1133.

Ozawa, I. On the tidal observation by means of a recording water-tube tiltmeter. *Journal of the Geological Society of Japan*, 1967, 12: 151-156.

Ponomarev, E.A.; and Sorokin, A.G. Infrasonic waves in the atmosphere over east Siberia. *Institute of Solar-Terrestrial Physics SD RAS*, 1996.

Posmentier, E. S. A theory of microbaroms. *Geophysical Journal International*, 1967, 13.5: 487-501.

Rhie, J.; and Romanowicz, B. Excitation of Earth's continuous free oscillations by atmosphere–ocean–seafloor coupling. *Nature*, 2004, 431.7008: 552-556.

Tanimoto, T. Continuous free oscillations: atmosphere-solid earth coupling. *Annual Review of Earth and Planetary Sciences*, 2001, 29.1: 563-584.

Tanimoto, T. Excitation of normal modes by atmospheric turbulence: source of long-period seismic noise. *Geophysical Journal International*, 1999, 136.2: 395-402.

Wenzel, H.-G. The nanogal software: Earth tide data processing package ETERNA 3.30. *Bull. Inf. Marées Terrestres*, 1996, 124: 9425-9439.

Received: *2022-05-11*

Reviewed: *2022-07-18 (undisclosed name); 2022-08-17 (P. Varga)*

Accepted: *2022-12-02*

SUPPLEMENTARY MATERIAL

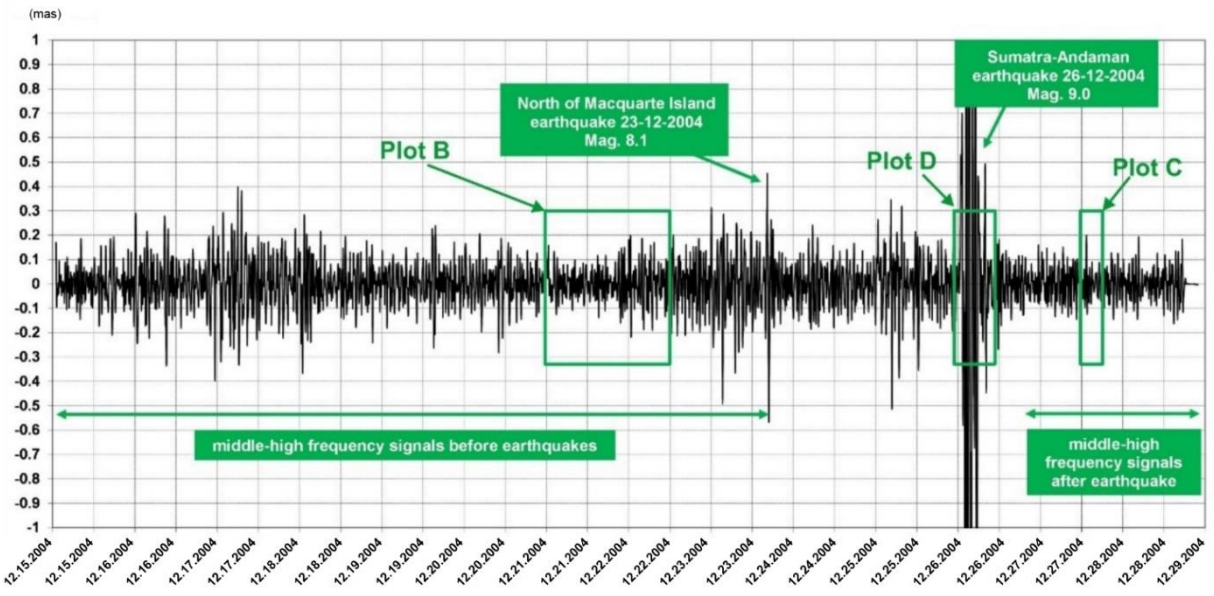

Figure 1S, plot A. Detailed plot of the signals in the range 10^{-3}–10^{-4} Hz observed in Channel No. 02 before, during, and after the earthquakes

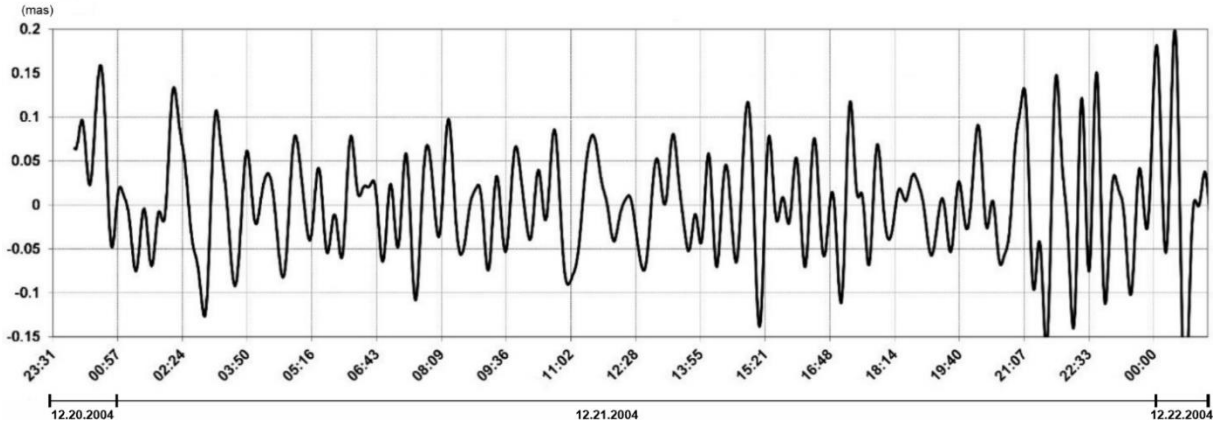

Figure 1S, plot B. Detailed plot of the signals in the range 10^{-3}–10^{-4} Hz observed in Channel No. 02 before, during, and after the earthquakes

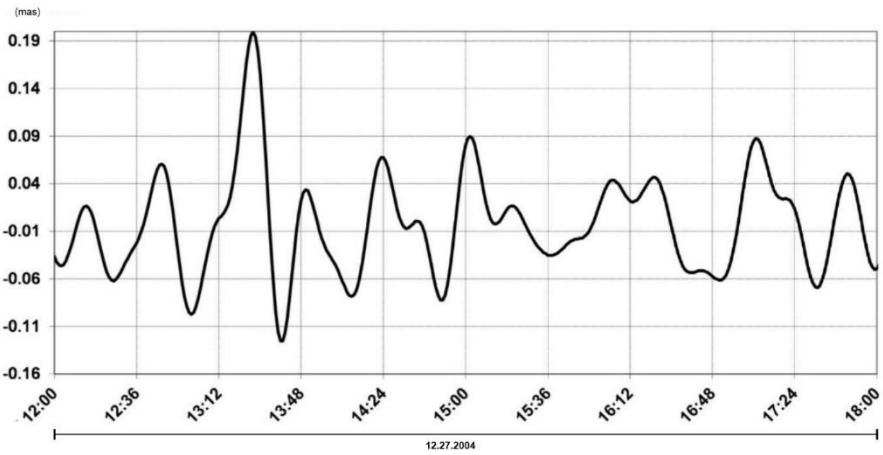

Figure 1S, plot C. Detailed plot of the signals in the range 10^{-3}–10^{-4} Hz observed in Channel No. 02 before, during, and after the earthquakes

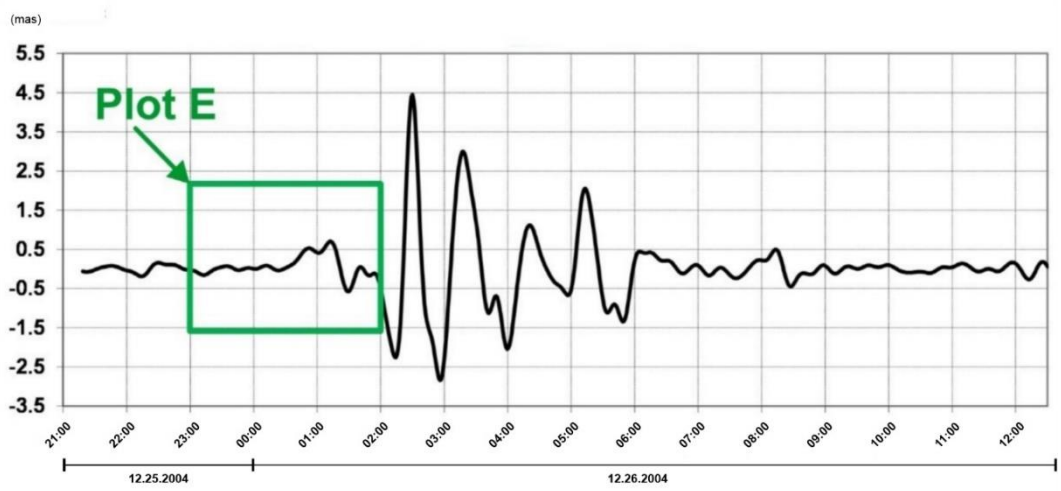

Figure 1S, plot D. Detailed plot of the signals in the range 10^{-3}–10^{-4} Hz observed in Channel No. 02 before, during, and after the earthquakes

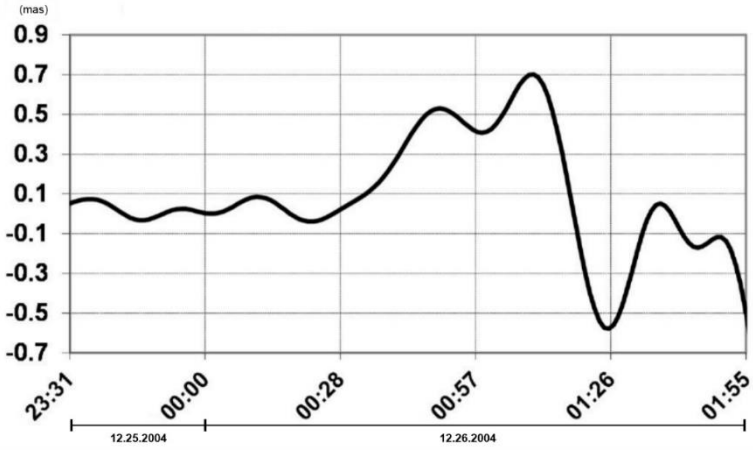

Figure 1S, plot E. Detailed plot of the signals in the range 10^{-3}–10^{-4} Hz observed in Channel No. 02 before, during, and after the earthquakes

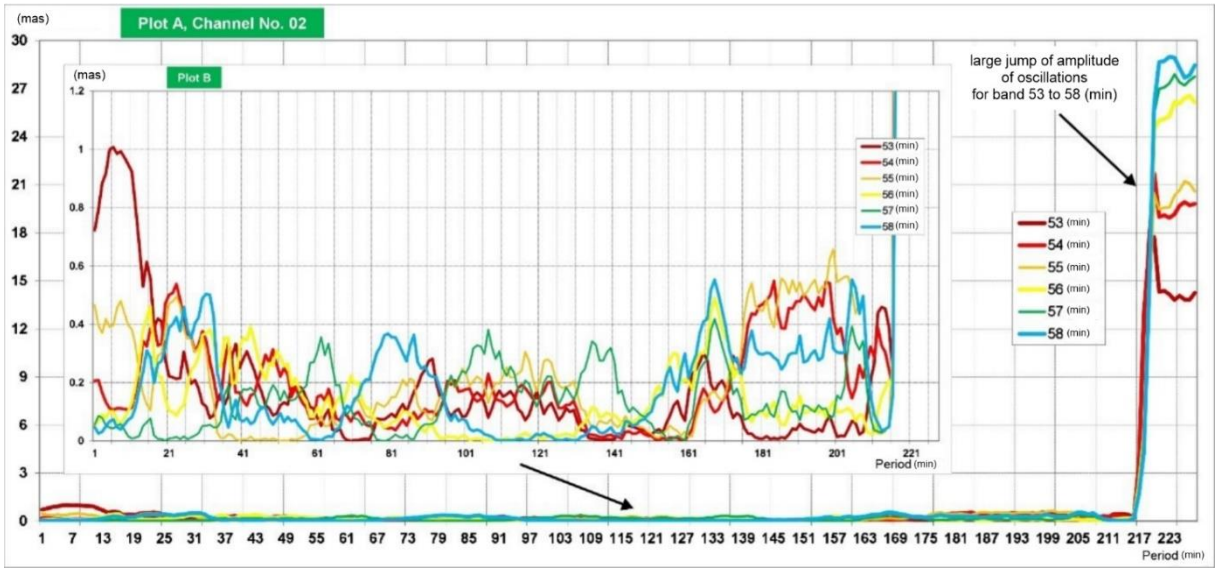

Figure 2S. Variability of amplitudes of the signals in the period range 10–100 min in Channel No. 02 in the time periods of 53–58 min in December 2004

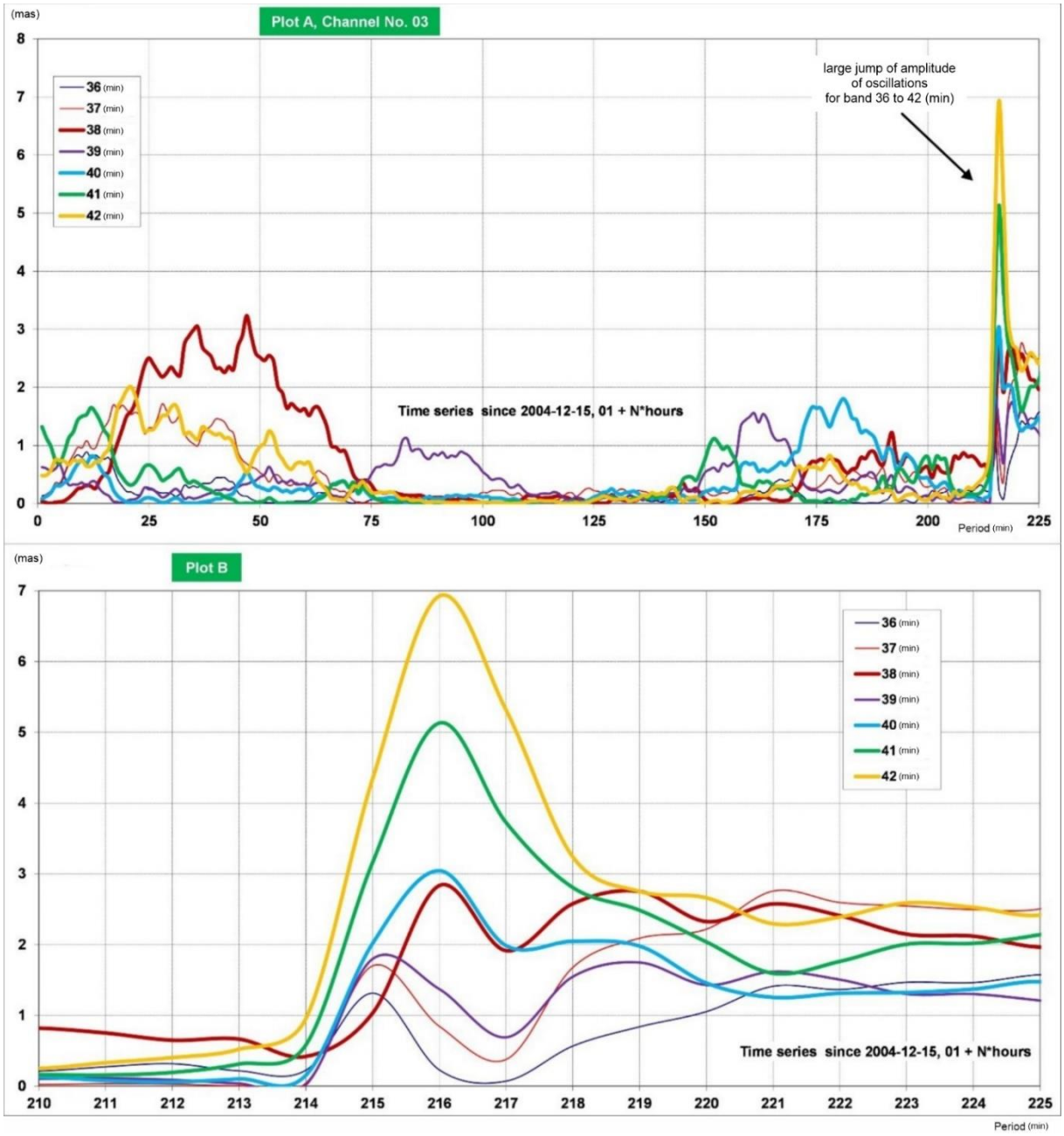

Figure 3S. Variability of amplitudes of the signals in the period range 10–100 min on Channel No. 03 in the period of 36–42 min in December 2004

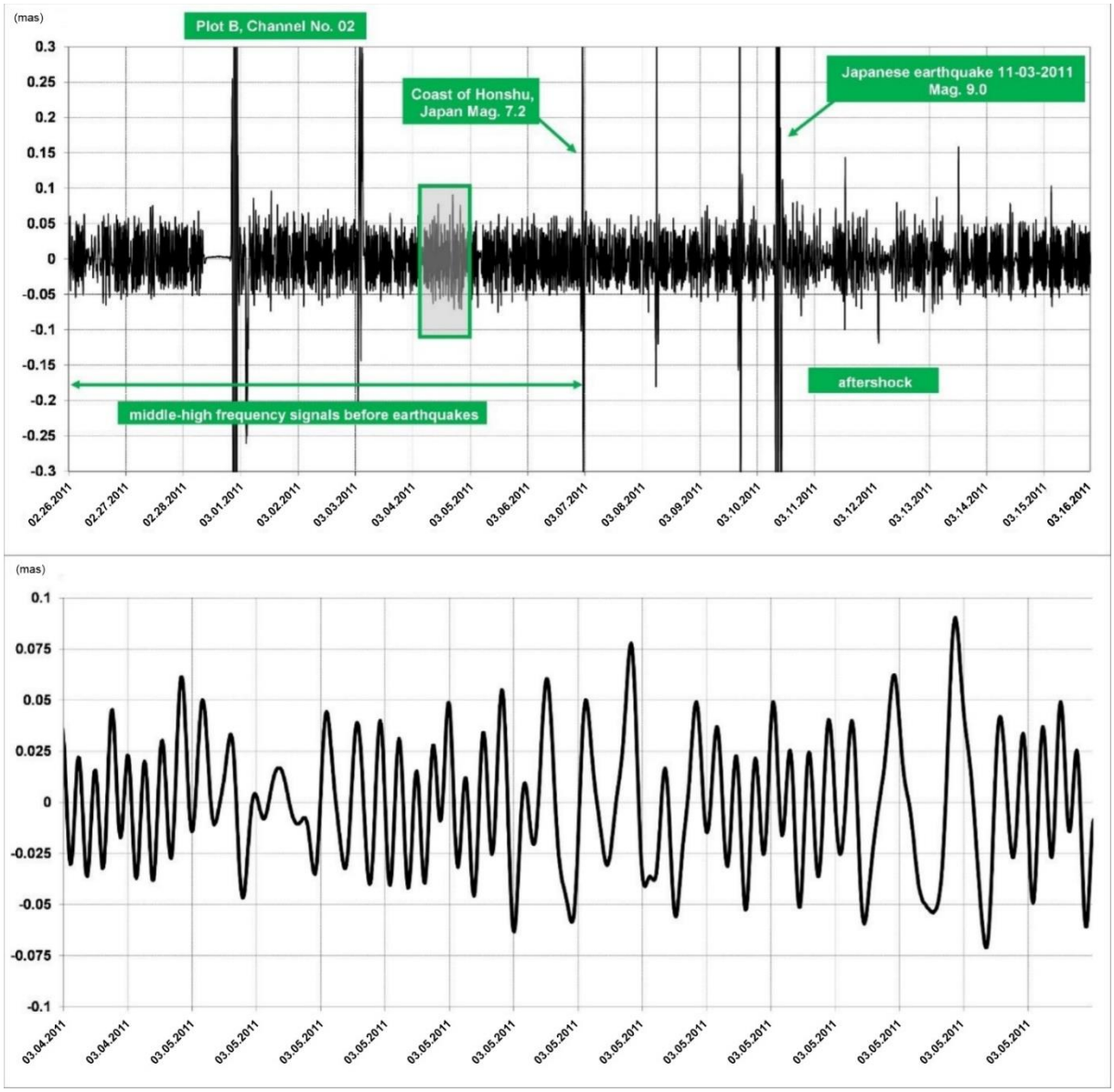

Figure 4S. Signal of the range 10^{-3}–10^{-4} Hz registered by the WTs in Channel No. 02 in March 2011

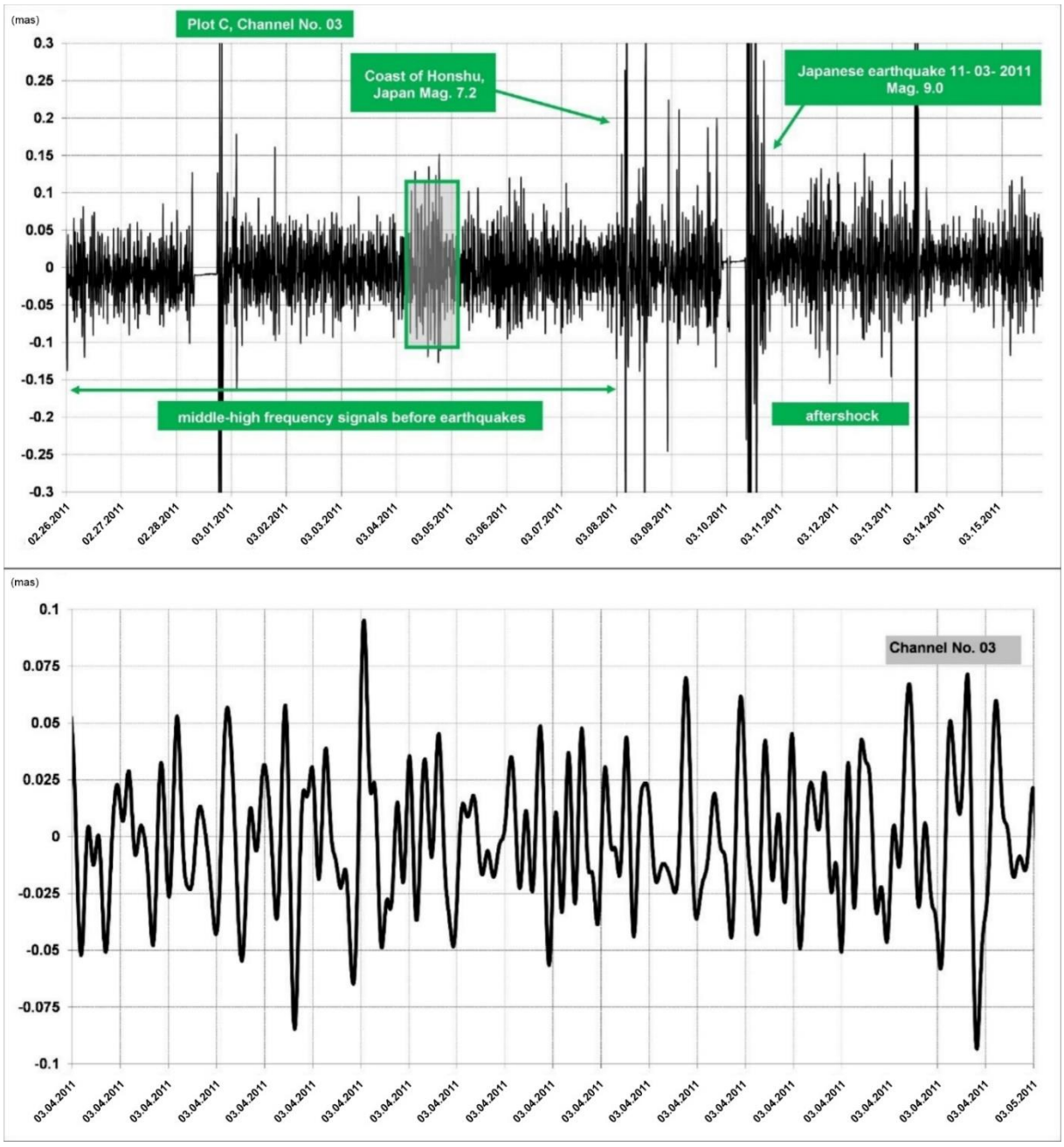

Figure 5S. Signal of the range 10^{-3}–10^{-4} Hz registered by the WTs in Channel No. 03 in March 2011

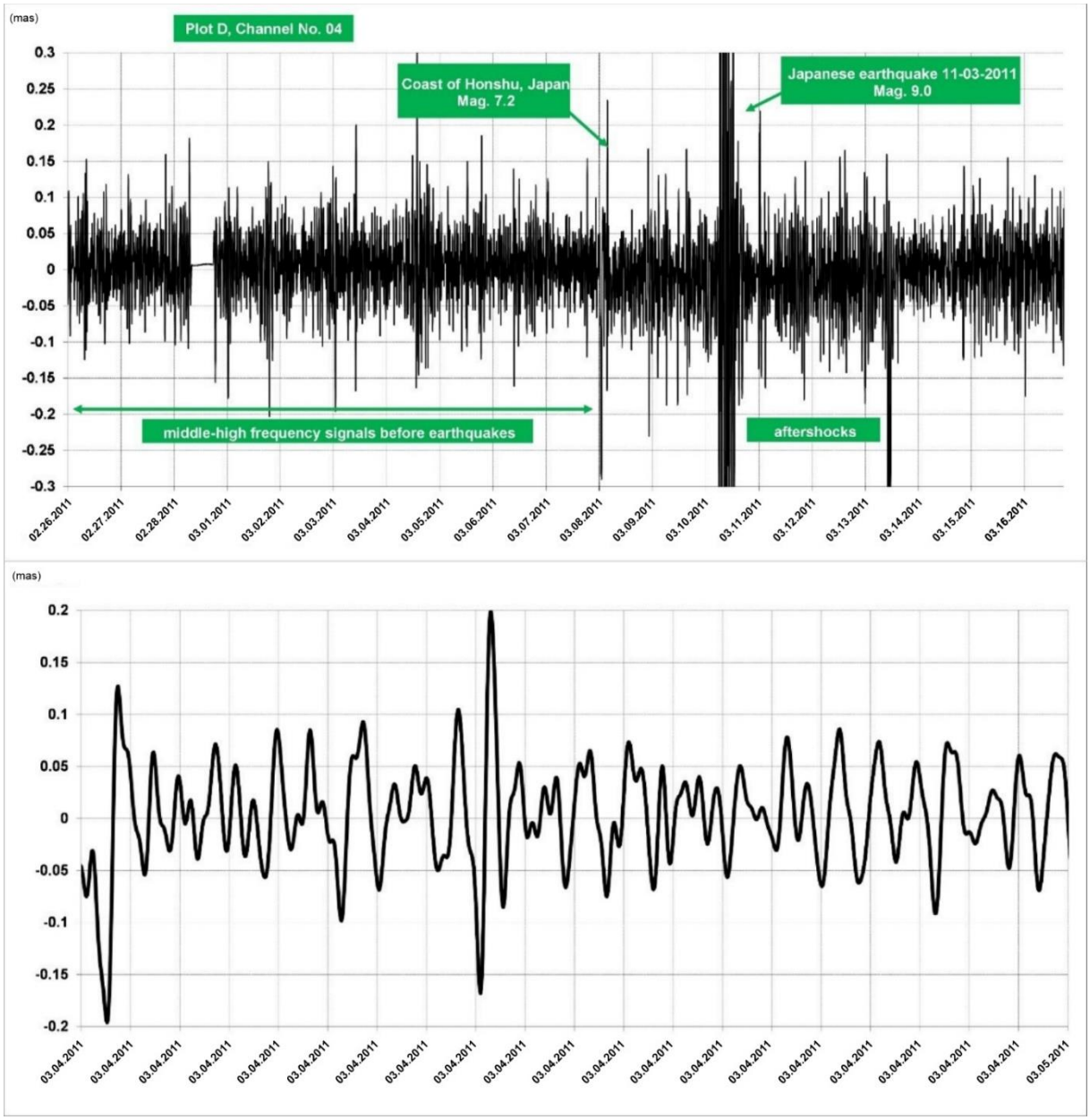

Figure 6S. Signal of the range 1 0^{-3}–10^{-4} Hz registered by the WTs in Channel No. 04 in March 2011